

Histological and Immunohistochemical Effects of Neuroectodermal cells Transplantation after Spinal Cord Injury in Rats

Saleh Al-Karim^{1,3}, **Wafaa S. Ramadan**^{2,3,4}, **Ghada A. Abdel-Hamid**^{2,3,5}, **Fatma Al Qudsi**^{1,3}

¹ Department of Biological Sciences, Faculty of Science, King Abdulaziz University, Jeddah, Saudi Arabia

² Department of Anatomy, Faculty of Medicine, King Abdulaziz University, Jeddah, Saudi Arabia

³ Embryonic Stem Cell Unit, King Fahd Medical Research Center, King Abdulaziz University, Jeddah, Saudi Arabia

⁴ Department of Anatomy, Faculty of Medicine, Ain Shams University, Cairo, Egypt

⁵ Department of Anatomy, Faculty of Medicine, Suez Canal University, Ismailia, Egypt

Running head: Neuroectodermal Transplantation in Spinal Cord Injury in Rats

*** Correspondence address:**

Ghada Abdel-Haye Abdel-Hamid,
Associate Professor of Anatomy,
Faculty of Medicine
King Abdullaziz University,
Jeddah 21551 KSA, P.O. Box: 42806;
E-mail: gmohamed@kau.edu.sa

Abstract

Background: In spinal cord injury, radical treatment is still a persistent hope for patients and clinicians. Our study aimed to determine the different histological changes in central, cranial and caudal sites of compressed spinal cord as a result of neuroectodermal stem cells (NESCs) transplantation in rats. **Material and methods:** For extraction of NESCs, future brains were extracted from mice embryos (10-days old) and cultured. Eighty, male rats were divided randomly into control, sham (20 rats each); while 40 rats were subjected to compressed spinal cord injury (CSCI). Seven days after spinal cord injury, rats were subdivided into 2 groups (20 rats each); an untreated and treated with NESCs injected cranial and caudal to the site of the spinal cord injury. Rats were sacrificed 4 weeks after transplantations of NESCs and specimens from the spinal cord at the central, cranial and caudal to site of spinal cord injury were proceeded to be stained with haematoxylin & eosin, osmic acid and Immunohistochemistry of glial fibrillary acidic protein (GFAP). **Results:** Sections of CSCI revealed areas of hemorrhages, necrosis and cavitation limited by reactive astrocytosis, with upregulation of GFAP expression. Evidence of remyelination and mitigation of histopathological features, reactive astrocytosis in CSCI sections were more pronounced in cranial than in caudal region. **Conclusions:** NESCs transplantation ameliorated the pathological changes, promoted remyelination.

Key words: neural, stem cells, compressed, spinal cord, injury, regeneration, rat

Introduction

Spinal cord injury (SCI) induced by trauma is a main health problem, with thousands of new cases reported each year. With the development of new advanced transportation methods, the rate of SCI has amplified. SCI is an important cause of mortality and morbidity [1]. SCI resulted in a loss of motor and sensation control, and hence affect the quality of life of the patient [2]. In Saudi Arabia, the average duration of inpatient rehabilitation programs for SCI ranges from one to one hundred and twenty weeks of hospitalization. The cost of these injuries to both individuals and to society is staggering [3]

Furthermore, management of SCI patients is puzzling. Noticeable motor and sensory impairment can result in long-life morbidity with a loss of voluntary control of urination and defecation, as well as the loss of a normal sexual life in males. SCI lead to several health problems and complications, as frequent kidney stones, urinary tract infections, respiratory and cardiac

dysfunctions and pressure sores [4]. These complications limit self-care and independence and make rehabilitation more difficult. The treatment of such complications is also very expensive [5].

The current treatment choices are physiotherapy and surgery, but as yet there is no therapy to entirely restore function. Stem cells are able to self-renewal and have the capability to differentiate to several cell types [6]. Stem cells are transplanted to stimulate repair after SCI. The transplanting stem cells can bridge axons in the damaged region, inducing stem cells to form oligodendrocyte precursors to remyelinate damaged axons [7]. Various types of cells have been used, but neuroectodermal cells have proved most acceptable for the regeneration of nervous tissue. Neuroectodermal stem cells (NESCs) differentiated to a various cells in nervous system, and so can be used for nerve injury treatment [8]. Several clinical trials have shown that cell. Transplantation is generally possible, but the efficiency of the method and the long-term care needs remain unconfirmed [9]. NESCs can live repeated freeze–bank–thaw cycles, and can preserve a normal karyotype and differentiation for years [6]. The aim of this study was to determine the possible regenerative effect of NESCs on the histological changes resulting from compressed injury to the spinal cord in a rat model.

Materials and Methods

Animals used in this study were mice for production of neuroectodermal stem cells and adult male rats for control, sham, SCI model and received transplanted NESCs. Both mice and rats were purchased from the animal house of King Fahd Medical Research Center, King Abdulaziz University, and Jeddah, Saudi Arabia. All techniques were conducted according to the guidelines of the Canadian Council on Animal Care. The rats were housed at 22–24°C, with a 12:12 light:dark photoperiod. The rats were fed a commercial diet and given water ad libitum.

I. Extraction of neuroectodermal stem cells

Forty female mice were mated overnight. Positive vaginal plugs were designated Day 0. The females were scarified on day 10 and the fetuses were surgically removed from the uterine horns and placed into phosphate buffered saline (Fig.1A). The fetuses were decapitated under a dissecting microscope with a scalpel and fine forceps (Fig.1B). The fetal heads were washed with phosphate buffered saline and 0.5% trypsin was added. The tissue was digested for 1 h at 37 °C then, 1 ml of phosphate buffered saline containing 0.04% deoxyribonuclease was added to the tissue. The resultant solution was aliquoted in 0.5-ml lots to 100-mm dishes containing 6 ml of a 1:1 mixture of Dulbecco's modified Eagle's medium and F12 medium (DME/ F 12) supplemented with 10% fetal bovine serum [10].

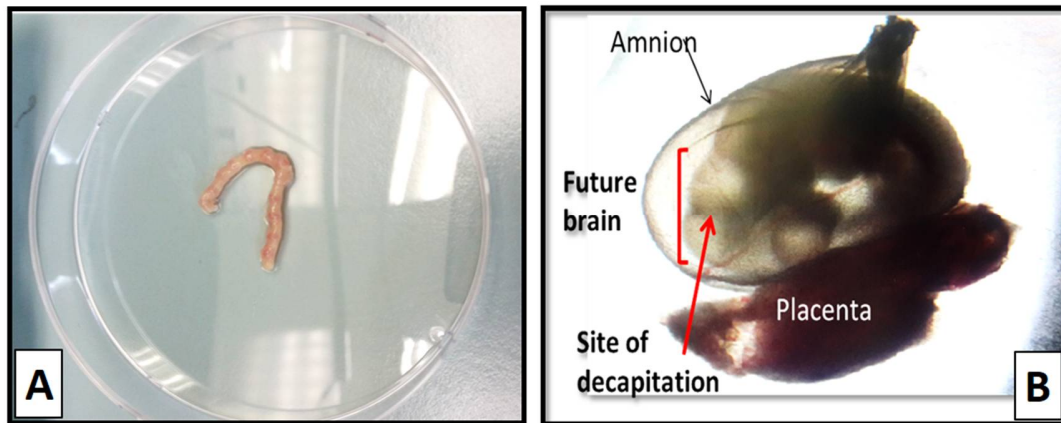


Figure 1: **A:** Photograph of a single uterine horn of a pregnant mouse loaded with ten-day-old embryos. **B:** Photograph of a ten-day-old mouse embryo for brain-tissue extraction.

II. Primary culture of embryonic neuroectodermal cells

Cells from approximately 10 fetal heads incubated for 7 h at 37 °C in humidified 5% CO₂:95% air. The majority of single cells spread and attached to the dish surface. These cells were like spindle-shaped fibroblasts. On the other hand, the spherical clusters of cells demonstrating the neural precursor cell population persisted floating. Isolated neural precursor cells from the 10 day-old mouse embryos were permitted to spread and attach to a plastic substrate and remain suspended in the culture medium. The fibroblastic cells' growth was inhibited in a selective medium. Cell proliferation amplified from day 0 to day 3, 7 days in culture [10]. Ten hours after incubation, the neural precursor cells appeared bright, loosely attached, and floating in the media, while the fibroblasts were attached to the plate surface (Fig. 2A) three days after clusters of NESCs were noticed (Fig. 2B).

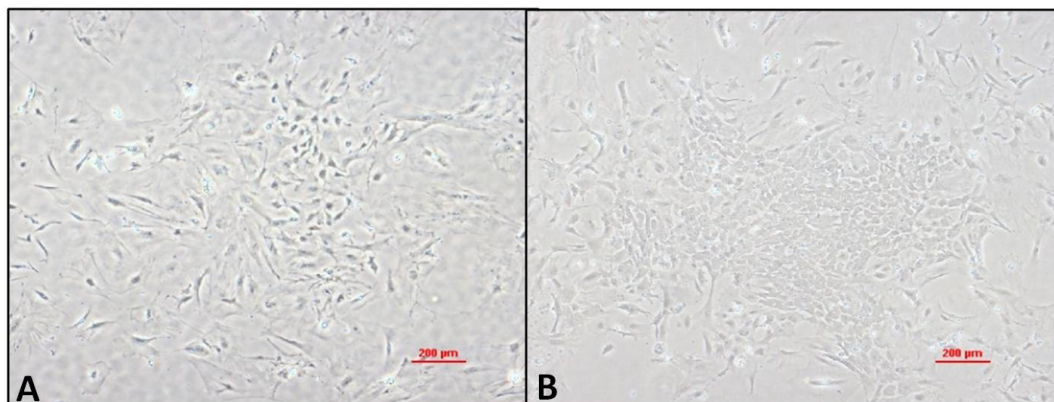


Figure 2: Photomicrograph showing isolation and initiation of the neuroectodermal stem cells (NESCs) from a ten-day-old mouse embryo head by trypsinization; plate (A) reveals the brightly loosely attached NESCs after ten hours; plate (B) shows clusters of NESCs after three days; scale bars = 200 μm

III. Formation of the CSCI model

Sixty male white Wistar rats weighing 200–250g were used. The animals were injected intraperitoneally by 7.5 mg/kg ketamine (Phoenix Pharmaceutical, St. Joseph, MO) and 60 mg/kg xylazine (Phoenix Pharmaceutical). The dorsal area between the neck and hind limbs, and extending 2 cm bilaterally from the spine, was shaved and disinfected with serial povidone and 70% ethanol scrubs. A midline incision exposed the spinal column at the level of T8–T11, and the paravertebral muscles were dissected bilaterally to visualize the transverse apophyses.

A laminectomy was performed at T10. The spinal cord injury was performed using a clip compression technique, described in [11]. The spinal cord was exposed, and except for the sham group, SCI was induced using a temporary aneurysm clip (Mizuho Aneurysm Clip, Mizuho, Japan) for 60 seconds. The deep and superficial muscle layers were sutured, and the skin was closed with stainless-steel wound clips. Immediately after surgery, animals were given subcutaneous saline and prophylactic Baytril (2.5 mg/kg/d, s.c.; Bayer, Shawnee Mission, KS) and maintained on an isothermic pad until alert and mobile. Manual bladder emptying technique twice daily was applied [12]. Antibiotics (enrofloxacin, 2.5 mg/kg) were given before surgery and daily for 3–5 days.

V. Transplantation of embryonic neuroectodermal and ESCs cells in CSCI

Seven days after compression of spinal cord twenty rats were left untreated (CSCI) the other twenty rats were treated by transplantation of NESCs. Only populations with over 95% viability were transplanted. Animals received cyclosporine as an immunosuppressive one day before and two days after transplantation. The animals were anesthetized as above and the laminectomy site was re-exposed (Fig.3A). A 10- μ l Hamilton syringe (Hamilton, Reno, NV) with a silicon-coated pulled glass tip was lowered into the spinal cord (Fig. 3B). Cell suspensions of neuroectodermal cells were injected along the midline of the spinal cord at a depth of 1.2 mm into one site 4 mm cranial to the lesion epicenter and into another site 4 mm caudal to the lesion epicenter, in a total volume of either 2.5 μ l (250,000 cells) at a rate of 2 μ l/min. The needle was removed after 5 min.

All rats in control, sham, CSCI and treated with NESCs were scarified after four weeks. Samples were taken of spinal cord tissues from all groups from central, cranial, and caudal to the site of spinal cord injury. The spinal cord tissues were removed rapidly, sliced coronal at 2 mm intervals and proceeded to all the subsequent histological and immunohistochemical evaluations.

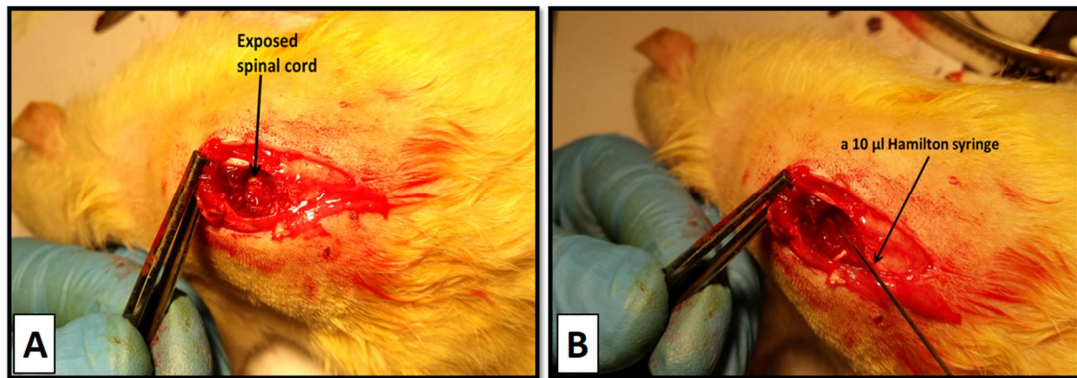


Figure 3: A: Photograph of a SCI rat model showing exposed spinal cord after laminectomy. B: Photograph showing transplantation of embryonic neuroectodermal cells into CSCI rat model using a 10- μ l Hamilton syringe.

A. Light microscopy studies

Specimens were fixed in 10% formalin and processed, embedded in paraffin wax. The 4- μ m-thick sections were stained with hematoxylin and eosin (H&E) examined using an Olympus BX51TF light microscope (Olympus, Tokyo, Japan), and photographed [13].

B. Immunohistochemistry of glial fibrillary acidic protein (GFAP)

The tissue sections were deparaffinized and dipped in phosphate-buffered saline, kept in cold methanol at 2 °C for 4 min, and washed in phosphate-buffered saline several times. The tissues were treated for 30 min with 3% H₂O₂, the primary antibody, rabbit anti-GFAP diluted 1:20 in phosphate-buffered saline was added. The tissues were then incubated for 1 h. For control, the primary antibody was omitted before adding the secondary antibody, biotin anti-rabbit, which was diluted 1:20 in phosphate-buffered saline containing 1% bovine serum albumin for 30 min. Then adding the extra avidin-peroxidase diluted 1:20 in phosphate-buffered saline containing 1% BSA for 30 min. The slides were then washed in phosphate-buffered saline and treated with diaminobenzidine for 30 seconds. Finally, the slides were washed in distilled water, dried, placed in xylene for 5 min, and mounted with DPX [14].

C. Quantitative analysis of glial fibrillary acidic protein expression

The slides were digitized using an Olympus digital camera installed on an Olympus BX51TF microscope with a $\times 1/2$ photo adaptor using a $\times 40$ objective. The resulting images were analyzed on an Intel Core I3-based computer using Video Test Morphology software (Video Test, St. Petersburg, Russia) with a specific built-in program for immunostaining analysis. The system measured the percentage area of GFAP-positive expression. The software routine for quantification was according to [15].

D. Osmic acid staining

The spinal cord sections (1 cm) were fixed with 4% paraformaldehyde for 24–48 h (at 4 °C) and dehydrated with 30% sucrose overnight (4 °C). Afterwards the specimens were removed from 4% paraformaldehyde, and each was rinsed with 0.01 mol/L phosphate-buffered saline for 20 min. They were transferred to 1% osmic acid for 3 to 7 days, and then rinsed with 0.01 mol/L phosphate-buffered saline and stored in 75% ethanol. This was followed by gradual alcohol dehydration and embedding in paraffin. The blocks were cut into sections using a conventional microtome (Leica CM1900, Leica Camera AG, Oskar-Barnack, Germany) [16].

Statistical analysis:

The data were statistically analyzed using SPSS statistical software, version 19.0 (SPSS Inc., Chicago, IL, USA) for Windows. The results were presented as means \pm SDs. The differences between the data were analyzed using one-way ANOVA. Data was presented as means \pm standard deviations (SD). $P \leq 0.05$ was considered significant.

Results

III. Histopathological examination

H&E-stained sections of the spinal cord in the control group revealed normal histological structure (Fig. 4A). The sham group did not show marked differences from the control, as there was only an apparent increase in the astrocytes (Fig.4B). Seven days after CSCI, sections of the spinal cord revealed areas of cavitation surrounded by a demarcating rim of numerous astrocytes with intensely acidophilic cytoplasm and dark shrunken nuclei (Fig.4C). Other sections revealed localized areas of hemorrhage (Fig.4D). After transplantation of neuroectodermal stem cells, an obvious increase was seen in astrocytes central and caudal to the site of the injury (Fig.5B,C); cranial to the lesion, an increase in oligodendrocytes was noticed (Fig.5A). Caudal to the site of CSCI, numerous degenerate axons were observed (Fig.5C).

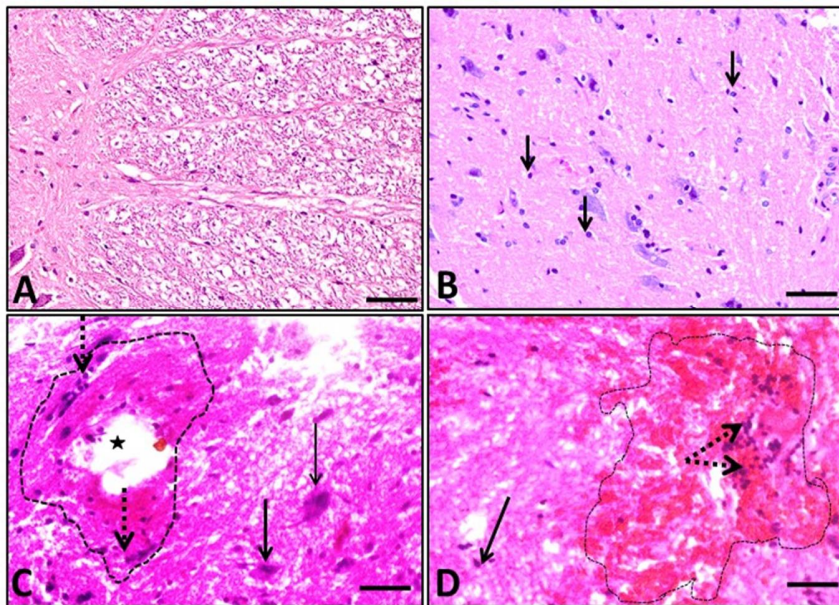


Figure 4: Sections of white matter of the spinal cord, as seen using (H&E) staining; note the normal structure in the control (A) and increased dispersed astrocytes (black arrows) in the sham group (B); (C): white matter of the spinal cord of rats, seven days after CSCI, showing areas of cavitation (star) surrounded by a demarcating rim of numerous astrocytes (dashed arrows), with intensely acidophilic cytoplasm and dark shrunken nuclei; note the large motor neurons (black arrows); (D): posterior horn of the spinal cord of rats seven days after the lesion, showing areas of localized hemorrhage with numerous astrocytes within the field (dotted arrows); small sensory neurons (black arrows); scale bars A–D, 50 μ m

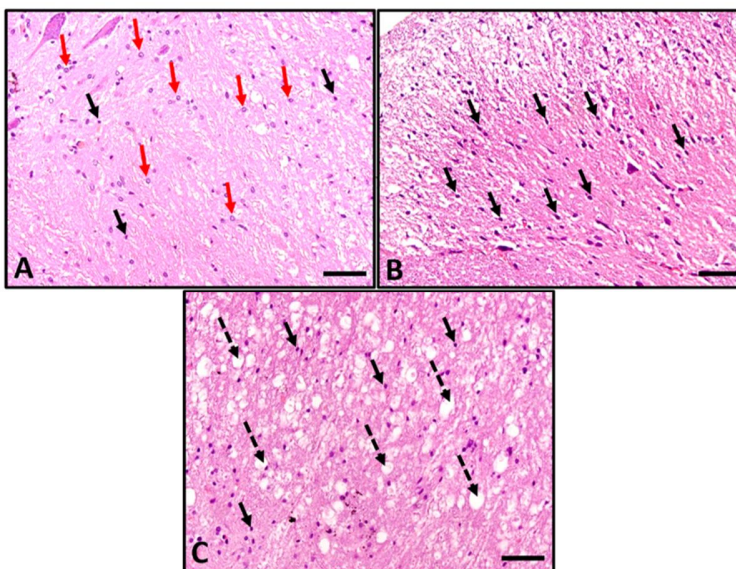


Figure 5: Sections of white matter of the spinal cord after transplantation of NESCs, as seen by (H&E) staining; A: cranial; B: central; C: caudal to the site of CSCI; an increase in astrocytes (black arrows) was noticed at sites central and caudal to CSCI; oligodendrocytes (red arrows) were observed in cranial sites; numerous degenerate axons (dotted black arrows) are visible caudal to the site of CSCI; scale bars A–C, 50 μ m

In immunostained sections with GFAP, the posterior funiculus of the white matter of the spinal cord of rats from the sham group showed an apparent increase in the scattered astrocytes, as compared to the control (Fig.6A,B). Seven days after CSCI, areas of reactive astrocytosis and numerous astrocytes with thick cytoskeletal processes were noticed, indicating an upregulation of GFAP expression (Fig.6C). After transplantation of the NESCs, normal distribution of the astrocytes in cranial and caudal to CSCI was seen (Fig.7A,C). Marked reactive astrocytosis with thick cytoskeletal processes was noticed in the area central to the CSCI (Fig.7B). The percentage of the mean area of GFAP expression increased significantly in CSCI and NESCs-treated groups (central to CSCI), as compared to control and sham groups (Fig.8).

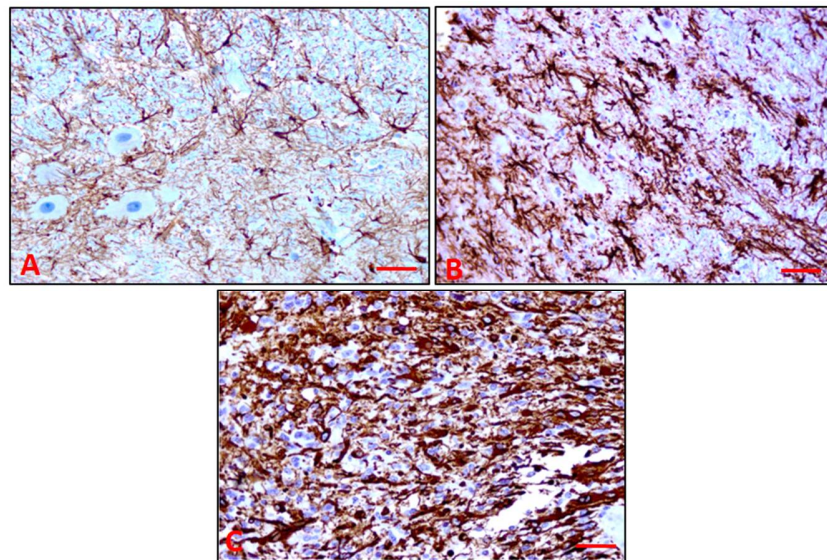


Figure 6: GFAP-immunostained sections of white matter from the spinal cord of the control group showing normal distribution of astrocytes (A) and apparent astrocytosis in the sham group (B); marked reactive astrocytosis with thick cytoskeletal processes (C) was visible seven days after CSCI; scale bars A–C, 50 μ m

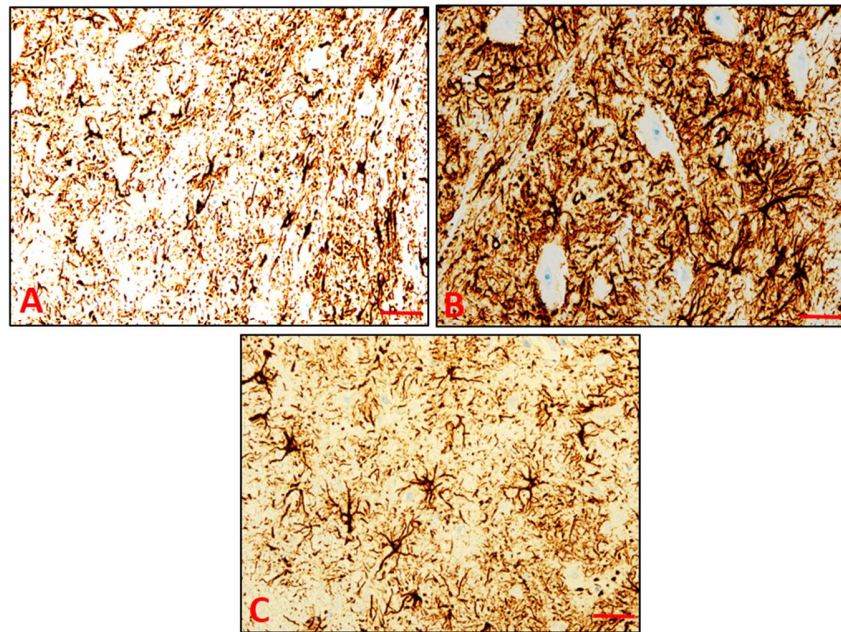


Figure 7: GFAP-immunostained sections of white matter from the spinal cord after transplantation of NESCs, showing normal distribution of the astrocytes cranial (A) and caudal to CSCI (C); marked reactive astrocytosis with thick cytoskeletal processes was noticed in the area central to the SCI (B); scale bars A–C, 50 μ m.

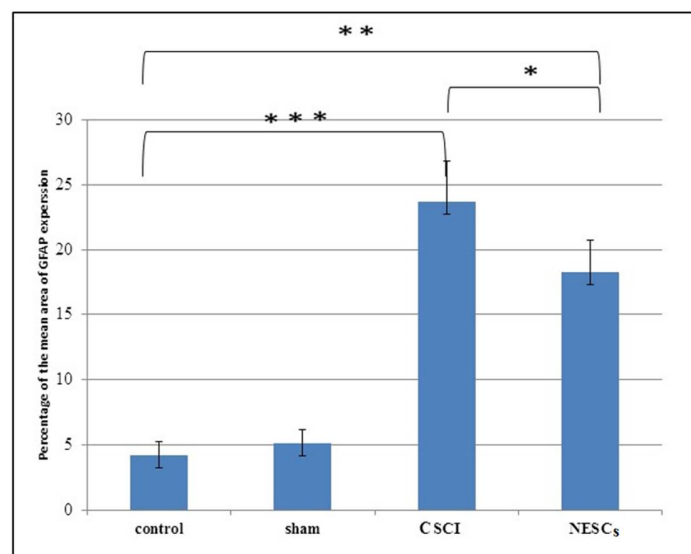


Figure 8: A bar graph showing the percentage of the mean area of GFAP expression in the control, sham, CSCI groups and NESCs-treated groups (central to CSCI); a one-way analysis of variance (ANOVA) test was used; data are presented as means \pm standard deviations (SD);

* $P \leq 0.05$: comparison between NESCs-treated group and CSCI;

** $P \leq 0.05$: comparison between NESCs-treated group and control and sham groups;

*** $P \leq 0.05$: comparison between CSCI and control and sham groups

The sections of the spinal cord stained with osmic acid revealed darkly stained intact myelin sheaths reflecting normal myelination of nerve fibers in the control and sham groups (Fig.9A,B). Seven days after CSCI, the nerve fibers were lost and the number of myelinated nerve fibers appeared to be minimal (Fig.9C). Transplantation of NESCs resulted in the regeneration of new myelinated nerve fibers, centrally and cranially to the site of the lesion (Fig.10A,B). Degenerated axons were noticed caudal to the site of spinal cord injury (Fig.10C).

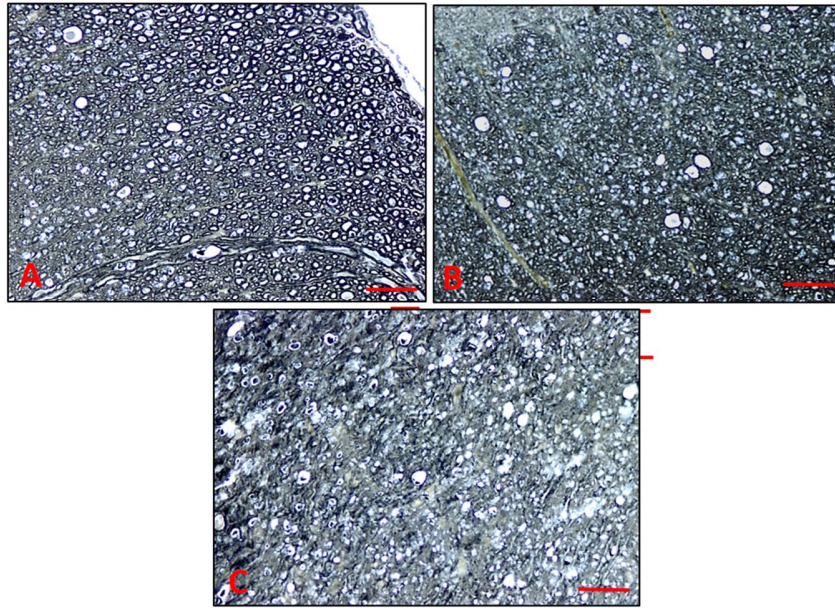


Figure 9: Sections of white matter from the spinal cord of the control (A) and sham (B) groups, as seen by staining with osmic acid, revealing darkly stained intact myelin sheaths; seven days after CSCI, nerve fibers were lost, and the number of myelinated nerve fibers appeared to be minimal (C); scale bars A–C, 50 μ m

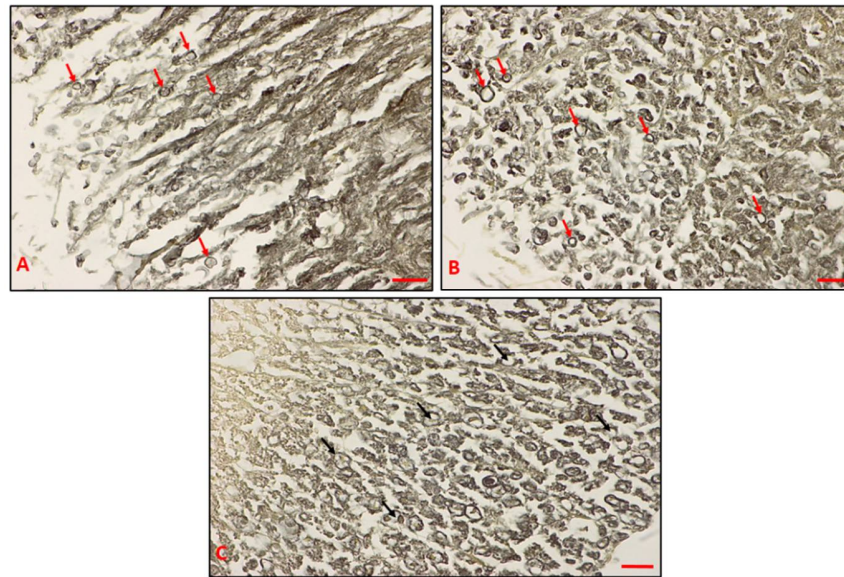


Figure 10: Sections of white matter of the spinal cord after transplantation of NESCs, showing new myelinated axons (red arrows) in cranially (A) and centrally (B) to the site of CSCI, and few caudally; scale bars A–C, 20 μ m

Discussion

Central nervous system injuries, such as SCI, results primarily from trauma, and can lead to loss of function and paralysis [17, 18]. Unfortunately, SCI has no proper treatment. In recent times, renewed attention has been given to finding and developing a complete treatment for SCI. In addition to neuroregenerative, neuroprotective, and neurocomputational strategies, cellular transplantation is considered the most relevant, inspiring, and encouraging therapy for SCIs [6].

Neural regeneration is a promising area of clinical practice and of theoretical research in neuroscience, particularly when no efficient treatment for neural damage has yet been developed. Accordingly, research into the transplantation of neural stem cells has gained a great deal of attention in medical research[4,19,20].

Neural stem cells (NSCs) have unique abilities not possessed by neurons, such as ease of collection, easy techniques for culturing and amplification, and the viability of autologous grafting after in vitro amplification, without encountering immune rejection. Neural stem cell transplantation has already been reported to be effective in treating nervous system injuries [21]. NSCs are easily collected and transported, and are well-matched with diverse delivery methods [22]. Moreover, NSCs can differentiate into astrocytes and neurons in vivo and in vitro [23]. Promising results after injection NSCs have been reported in the treatment of amyotrophic lateral sclerosis in humans [24].

In the present study, the compression model for SCI model was chosen to determine the efficacy of neuroectodermal stem cells in the treatment of CSCI. The compression model was selected to mimic the ventral compression that is seen in human clinical settings [25]. Hence, compression and contusion models are more clinically applicable [26].

In the current study, seven days after CSCI, areas of localized hemorrhage and fibrinoid necrosis were observed at the site of injury. Ischemia, hemorrhage, systemic hypotension, and microcirculatory disturbances are the vascular manifestations of CSCI. A major decrease in blood flow occurs immediately after SCI at the lesion site [27], while ischemia worsens in the first few hours [28]. After a period of ischemia, blood reperfusion occurs, with increased free radicals that lead to paradoxical reperfusion damage [29]. The disruption of small blood vessels and hemorrhage affects local microcirculation more than large arteries, which leads to a failure of glutamate-mediated excitotoxicity and autoregulation.

Additionally, severe systemic hypotension increases microcirculation dysfunction and exacerbates injury [30]. This is accompanied by inflammation of the nervous tissue that influences the cells to become necrotic at the injured site. At this stage, various types of immune cell—including neutrophils, monocytes, microglia, and T-lymphocytes—secrete certain cytokines, such as tumor necrosis factor- α , interleukin-1 β , and interleukin-6, which leads to apoptotic cell death [31].

Reactive astrocytosis was noted seven days after CSCI, and confirmed by the significant increase in the percentage of the mean area of GFAP expression. It was reported that astrocytosis can suppress oligodendrocyte generation and prevent remyelination by secreting endothelin-1 [32]. Similarly, reactive astrocytes inhibit neural axon regeneration after SCI in mice [33]. On the other hand, previously found that reactive astrocytes restricted leukocyte infiltration, repaired the blood-brain barrier, and preserved motor function [14]. Furthermore, demyelination was a consistent histopathological feature in osmic acid stained sections at the site of the lesion seven days after CSCI.

In the present study, transplantation of NESCs led to decrease in hemorrhage area and zones of cavitation in the examined H&E stained sections. The most important observed result is the remyelination occurring at the site of transplantation. Moreover, the cranial region also revealed mitigation of the pathological features noted in case of CSCI. On the other hand the caudal region, compared to the cranial segment, did not show significant improvement. The enhancement of the astrocytes expressed by the increase in the area percentage of the GFAP, noted at the site of the lesion, suggests that NESCs were able to differentiate into glial astrocytes. This was confirmed by a previous study which proposed that activated astrocytes have positive effects on myelination and can promote the percentage of myelinated fibers in CNS rat cultures [34]. It has been suggested that the increase in IL-1 β levels at early stages of central nervous system pathology stimulates the induction of mRNA, and protein in astrocytes, a phenomenon which appears to be important for remyelination [35].

Conclusion

Understanding the detailed pathology of CSCI would facilitate more complicated procedures in future. The present work thus aimed to study the marked pathological changes in the CSCI models, compared with sham and control groups. It has been established that the NESCs alleviated histopathological changes that induced by CSCI and promoted remyelination. Further studies are needed to investigate the ultrastructural changes in spinal cord after CSCI and evidence of remyelination and restoration of locomotor function after transplantation of NESCs.

Acknowledgments

This study was supported by King Abdulaziz City for Science and Technology (KACST) by a research grant No. 133-35-أ.ت.

Conflict of Interest

The authors declare that they have no conflicts of interest regarding this study.

References

1. Ku, J.H. 2006: The management of neurogenic bladder and quality of life in spinal cord injury. *BJU Int.* 98: 739-745.
2. Beck, K.D., Nguyen, H.X., Galvan, M.D., Salazar, D.L., Woodruff, T.M., Anderson, A.J. 2010. Quantitative analysis of cellular inflammation after traumatic spinal cord injury: evidence for a multiphasic inflammatory response in the acute to chronic environment. *Brain.* 133: 433-447.
3. Al-Jadid, M.S., 2013. A retrospective study on traumatic spinal cord injury in an inpatient rehabilitation unit in central Saudi Arabia. *Saudi Med J.* 34(2):161–165.
4. Theus MH, Wei L, Cui L, Francis K, Hu X, Keogh C, Yu SP. 2008. In vitro hypoxic preconditioning of embryonic stem cells as a strategy of promoting cell survival and functional benefits after transplantation into the ischemic rat brain. *Exp Neurol.* 210:656–670.
5. Drigotaite N, Krisciūnas A. 2006. Complications after spinal cord injuries and their influence on the effectiveness of rehabilitation]. *Medicina (Kaunas).* 42(11):877-80. Review. Lithuanian.
6. Roy, R.R., Harkema, S.J., Edgerton, V.R. 2012. Basic concepts of activity-based interventions for improved recovery of motor function after spinal cord injury. *Archives of physical medicine and rehabilitation* 93:1487-1497.
7. Plemel JR, Keough MB, Duncan GJ, Sparling JS, Yong VW, Stys PK, et al. 2014. Remyelination after spinal cord injury: Is it a target for repair? *Prog Neurobiol.* 117:54–72.

8. Furuya T, Hashimoto M, Koda M, Okawa A, Murata A, Takahashi K, Yamashita T and Yamazaki M. 2009. Treatment of rat spinal cord injury with a Rho-kinase inhibitor and bone marrow stromal cell transplantation. *Brain Res* 1295: 192-202.
9. Assinck, P., Duncan, G. J., Hilton, B. J., Pleme, J. R., Tetzlaff, W. 2017. Cell transplantation therapy for spinal cord injury. *Nature neuroscience*. 20 (5):637-647.
10. Kitani H, Shiurba R, Sakakura T, Tomooka Y. 1991. Isolation and characterization of mouse neural precursor cells in primary culture. *In Vitro Cell Dev Biol*. 27A(8):615-24.
11. Bakar, B., Kose, E., Ayva, S.K., et al. 2013. Effects of low-dose methotrexate in spinal cord injury in rats. *Turk J Trauma Emergency Surg*. 19 (4): 285–293.
12. Liu, X.Z. et al. 1997. Neuronal and glial apoptosis after traumatic spinal cord injury. *J. Neurosci*. 17: 5395–5406.
13. Bancroft, J.D., Gamble, M. 2008. Hematoxylin and eosin, connective tissue and stain, carbohydrates. In: *Theory and practice in histological techniques*. 6th ed. Churchill-Livingstone, Edinburgh. Pp. 121–186.
14. Faulkner JR, Herrmann JE, Woo MJ, Tansey KE, Doan NB, Sofroniew MV. 2004. Reactive astrocytes protect tissue and preserve function after spinal cord injury. *J Neurosci*. 3;24(9):2143-55.
15. Wakasa S, Shiiya N, Tachibana T, Ooka T, Matsui, Y. 2009. A semiquantitative analysis of reactive astrogliosis demonstrates its correlation with the number of intact motor neurons after transient spinal cord ischemia. *J Thorac Cardiovasc Surg*. 137(4):983-90.
16. Di Scipio F1, Raimondo S, Tos P, Geuna S. A. 2008. Simple protocol for paraffin-embedded myelin sheath staining with osmium tetroxide for light microscope observation. *Microsc Res Tech*. 71(7):497-502.
17. Carvalho, K.A., Vialle, E.N., Moreira, G.H., Cunha, R.C., Simeoni, R.B., Francisco, J.C., Guarita-Souza LC, Oliveira L, Zocche L, Olandoski M. 2008. Functional outcome of bone marrow stem cells (CD45(+)/CD34(-)) after cell therapy in chronic spinal cord injury in Wistar rats. *Transplant Proc*. 40:845–846.
18. Sun Z, Wen Y, Mao Q, Hu L, Li H, Sun Z, Wang D. 2010. Adenosine-triphosphate promoting repair of spinal cord injury by activating mammalian target of rapamycin/signal transducers and activators of transcription 3 signal pathway in rats. *Zhongguo Xiu Fu Chong Jian Wai Ke Za Zhi*. 24:165–171. (In Chinese)
19. Bhang, S.H., Lee, Y.E., Cho, S.W., Shim, J.W., Lee, S.H., Choi, C.Y., Chang, J.W., Kim, B.S. 2007. Basic fibroblast growth factor promotes bone marrow stromal cell transplantation-mediated neural regeneration in traumatic brain injury. *Biochem Biophys Res Commun*. 359:40–45.
20. Hwang DH, Shin HY, Kwon MJ, Choi JY, Ryu BY, Kim BG. 2014. Survival of neural stem cell grafts in the lesioned spinal cord is enhanced by a combination of treadmill locomotor training via insulin-like growth factor-1 signaling. *J Neurosci*. 34:12788–12800.

21. Shen LH, Li Y, Gao Q, Savant-Bhonsale S, Chopp M. 2008. Down-regulation of neurocan expression in reactive astrocytes promotes axonal regeneration and facilitates the neurorestorative effects of bone marrow stromal cells in the ischemic rat brain. *Glia*.56:1747–1754.
22. Giordano A., Galderisi U., Marino I.R. 2007. From the laboratory bench to the patient's bedside: an update on clinical trials with mesenchymal stem cells. *J Cell Physiol*.211:27–35.
23. Jori FP, Napolitano MA, Melone MA, Cipollaro M, Cascino A, Altucci L, Peluso G, Giordano A, Galderisi U. 2005. Molecular pathways involved in neural in vitro differentiation of marrow stromal stem cells. *J Cell Biochem.* ;94:645–655.
24. Mazzini L, Mareschi K, Ferrero I, Vassallo E, Oliveri G, Nasuelli N, Oggioni GD, Testa L, Fagioli F. 2008. Stem cell treatment in Amyotrophic Lateral Sclerosis. *J Neurol Sci*. 265:78–83.
25. Onifer SM, Rabchevsky AG, Scheff SW. 2007. Rat models of traumatic spinal cord injury to assess motor recovery. *ILAR J*. 48(4):385-95.
26. Alhoseini, M.S., Movaghar, V.R., 2014. Orthopedics, Physical Medicine and Rehabilitation Animal Models in Traumatic Spinal Cord Injury. "Topics in Paraplegia", book edited by Yannis Dionyssiotis, ISBN 978-953-51-1621-9.
27. Tator C.H., Fehlings M.G. 1991. Review of the secondary injury theory of acute spinal cord trauma with emphasis on vascular mechanisms, *Journal of neurosurgery* 75(1) :15-26.
28. Oyinbo, C.A. 2011. Secondary injury mechanisms in traumatic spinal cord injury: a nugget of this multiply cascade, *Acta Neurobiol Exp (Wars)* 71(2): 281-99.
29. Lee S.M., Yune T.Y., Kim S.J., Park D.W., Lee Y.K., Kim Y.C., Oh Y.J., Markelonis G.J., Oh T.H. 2003. Minocycline reduces cell death and improves functional recovery after traumatic spinal cord injury in the rat, *Journal of neurotrauma*. 20(10): 1017-1027.
30. Xu G.-Y., Hughes M.G., Zhang L., Cain L., McAdoo D.J. 2005. Administration of glutamate into the spinal cord at extracellular concentrations reached post-injury causes functional impairments, *Neuroscience letters*. 384(3):271-276.
31. Bareyre, F.M., Schwab, M.E. 2003. Inflammation, degeneration and regeneration in the injured spinal cord: insights from DNA microarrays. *Trends in neurosciences*. 26(10): 555-563.
32. Hammond TR, Gadea A, Dupree J, Kerninon C, Nait-Oumesmar B, Aguirre A, Gallo V 2014 Astrocyte-derived endothelin-1 inhibits remyelination through notch activation. *Neuron* 81:588-602.
33. Menet V, Prieto M, Privat A, Gimenez y Ribotta M. 2003. Axonal plasticity and functional recovery after spinal cord injury in mice deficient in both glial fibrillary acidic protein and vimentin. *Proc Natl Acad Sci USA* 100:8999–9004.

34. Nash B., Thomson C.E., Linington C., Arthur A.T, McClure J.D., McBride M.W., Barnett S.C. 2011. Functional duality of astrocytes in myelination J. Neurosci., 31:13028-13038.
35. Liberto C.M., Albrecht P.J., Herx L.M., Yong V.W., Levison S.W. 2004. Pro-regenerative properties of cytokine-activated astrocytes. J. Neurochem., 89 :1092-1100